J. Cent. South Univ. (2015) 22: 1869−1877
DOI: 10.1007/s11771-015-2706-4

Springer

Mechanism of cement-stabilized soil polluted by magnesium sulfate

HAN Peng-ju(韩鹏举)[1, 2], WANG Shuai(王帅)[1], Frank Y. Chen(陈幼佳)[1, 2], BAI Xiao-hong(白晓红)[1]

1. College of Architecture and Civil Engineering, Taiyuan University of Technology, Taiyuan 030024, China;
2. Department of Civil Engineering, The Penn State University, Harrisburg, PA 17057, USA

Abstract: In order to simulate and study the mechanism of cement stabilized soils polluted by different contents of magnesium sulfate (MS), a series of tests were conducted on the cemented soil samples, including unconfined compression strength (UCS) tests of blocks, X-ray diffraction (XRD) phase analysis of powder samples, microstructure by scanning electronic microscopy (SEM), element composition by energy dispersive spectrometry (EDS), and pore distribution analysis by Image Processed Plus 6.0 (IPP 6.0) software. The UCS test results show that UCS of cemented soils reaches the peak value when the MS content is 4.5 g/kg. While, the UCS for Sample MS4 having the MS content of 18.0 g/kg is the lowest among all tested samples. Based on the EDS analysis results, Sample MS4 has the greater contents for the three elements, oxygen (O), magnesium (Mg) and sulfur (S), than Sample MS1. From the XRD phase analysis, C-A-S-H ($3CaO{\cdot}Al_2O_3{\cdot}3CaSO_4{\cdot}32H_2O$ and $3CaO{\cdot}Al_2O_3{\cdot}CaSO_4{\cdot}18H_2O$), M-A-H ($MgO{\cdot}Al_2O_3{\cdot}H_2O$), M-S-H ($MgO{\cdot}SiO_2{\cdot}H_2O$), $Mg(OH)_2$ and $CaSO_4$ phase diffraction peaks are obviously intense due to the chemical action associated with the MS. The pore distribution analysis shows that the hydrated products change the distribution of cemented soil pores and the pores with average diameter (AD) of 2−50 μm play a key role in terms of the whole structure of cemented soil. The microscopic structure of the cemented soil with MS exhibits the intertwined and embedded characteristics between the cement and granular soils from the SEM images of cemented soils. The microstructure analysis shows that the magnesium sulfate acts as the additive, which is beneficial to the soil strength when the MS content is low (i.e., Sample MS2). However, higher MS amount involving a chemical action makes samples crystallize and expand, which is adverse to the UCS of cemented soils (i.e., Sample MS4).

Key words: unconfined compression strength (UCS); magnesium sulphate (MS); X-ray diffraction (XRD); microstructure; energy dispersive spectrometer (EDS)

1 Introduction

Cement stabilized soil technique is a method of mixing the cement with in-situ soils in order to improve the soil properties. The reinforcing effectiveness becomes better when the soil contains clay minerals such as kaolinite or montmorillonite. On the other hand, the strength of cemented soils would be lower when the soil contains illite, which has a higher organic content, or is at a lower acidity (i.e., pH<7.0). Many researchers have studied the influence of environment on cemented soil properties. ROLLINGS et al [1] and BAI et al [2] tested the mechanical properties and electrical resistances of the cemented soils polluted by acid. SHITATA and BAGHDADI [3] investigated the durability characteristics and compressive strengths of cemented soils after an extended exposure to saline ground water. HUANG et al [4] studied cemented soils utilizing scanning electronic microscopy (SEM) images, discussed the form of micro-structure, and evaluated the micro-structure pore quantitatively. DONG et al [5−6] studied the influence of acid environmental contamination on cemented soil from the perspective of the electrical property of cemented soil. XING et al [7] indicated that magnesium ion, chloride, and sulfate ion caused the change in the microstructures of salt-rich soil-cements and reduced the strength of soil-cement composites. LIU et al [8] came up with the relationship between ion concentration and corrosion time based on the theory of chemical dynamics, damage mechanics, chemical reaction formula between the magnesium chloride and the cement soil, and certain assumption. HEINECK et al [9] analyzed the micro-structural behavior of composite mixtures of residual soils and sodic bentonites that were used as contaminant barriers. They carried out a series of micro-structural analysis including X-ray diffraction (XRD), scanning electronic microscopy (SEM), and energy dispersive spectrometry (EDS). Their results demonstrated that the non-cemented mixture was destructive after the percolation by alkaline liquids, while the cemented mixture remained stable

Foundation item: Projects(51208333, 51078253) supported by the National Natural Science Foundation of China
Received date: 2014−04−04; **Accepted date:** 2014−09−15
Corresponding author: BAI Xiao-hong, Professor; Tel: +86−351−6010976; E-mail: bxhong@tytu.edu.cn

without a major change. VOGLAR and LESTAN [10] developed a strength model in which the formulations of ordinary Portland cement (OPC), calcium aluminate cement (CAC), and pozzolanic cement (PC) with additives were used for solidification/stabilization (S/S) of soils from a contaminated industrial field. ZHA et al [11] utilized the unconfined compressive strength (UCS) test, leaching test, and SEM test to study the effects of cyclic wetting and drying on solidified/stabilized soils contaminated by fly ash and revealed the micro-mechanism of the variations of the engineering properties of stabilized contaminated soils. ZANDIEH and YASROBI [12] proved that two polymer materials could be used to stabilize the polluted soils on road shoulders and slopes, and these polymers improve the compressive strength from 0.03 MPa for control samples to 5.2 MPa for improved samples. WALKER and DOBSON [13−14] summarized the results from a comprehensive investigation undertaken to assess the influence of soil characteristics and cement content on the physical properties of stabilized soil blocks. NING et al [15−16] investigated the behavior of cemented soils under various environmental conditions and concluded that, contrary to the mechanical strength, the environmental erosion had little effects on the fracturing process. BLASCO et al [17] studied the ability of calcium aluminate cement (CAC) to encapsulate toxic metals under two curing conditions, in which the soil pore size distribution patterns were identified and related to the compounds as detected by XRD and SEM. YANG et al [18−19] considered the following factors: cement content, curing age, magnesium sulfate (MS) solution concentration, and pH value in their studies, and concluded that the strength of cemented soils increased with the cementing content and curing age. Polluted soil sites of MS were mainly from the industries of leather factory, paper mill, chemical and fertilizer plant, battery industry, and so on. If a cement stabilized soil technique is used for the polluted soil, such polluted soil environment would inevitably cause the cemented soil to change its mechanical property. Nevertheless, mechanism research related to the influence of MS on the properties of cemented soils is still rather limited. In order to further study the stabilized influence effect in MS polluted soil environment, techniques including UCS test, XRD, SEM, EDS, and pore distribution information analysis by Image Processed Plus 6.0 (IPP 6.0) software were considered. The relationships among UCS, element content, composite phase, microstructure, and pore distribution were studied. The concluding results may be considered as the pollution mechanism for cement stabilized soils.

2 Experimental procedures

2.1 Materials

1) Soil: Air dried silt soil with liquid limit water content (w_L) of 27.8%, plastic limit water content (w_P) of 19.0%, plasticity index (I_P or PI) of 8.8, uniformity coefficient (C_u) of 26.67, and curative coefficient (C_c) of 1.35 were used. Its main chemical compositions are listed in Table 1.

2) Cement: Ordinary Portland cement (OPC) with compressive strength of 32.5 MPa for 28 days of curing, produced by a local cement company in Taiyuan, China, was used.

3) Proportion of contents of cemented soil (CS): Soil:cement:water is 100:20:50.

4) Mass content of MS in cemented soil (CS) is 0, 1.5, 4.5, 9.0 and 18.0 g/kg. The mixing method for polluted soils using MS is to make the MS reagent into five different concentrations of solution. The general formula and code rule for CS are listed in Table 2.

5) Mixing machine: SJ-15 blender with body volume of 15 L and rotational speed of (80±4) r/min was used. Typical size of scaled CS samples is 70.7 mm×70.7 mm× 70.7 mm.

6) Standard curing time for the CS is 28 days.

7) Curing condition: Temperature is 20.9 °C; Relative humidity is 90.7%.

Table 1 Main chemical compositions of soil specimens (g/kg)

Ca^{2+}	Mg^{2+}	Cl^-	SO_4^{2-}	HCO_3^-	Soluble salt
0.154	0.101	0.11	0.216	0.138	1.72

Table 2 General formula and code for CS

Sample code	Concentration of MS solution/ ($g \cdot L^{-1}$)	MS content in polluted soil/($g \cdot kg^{-1}$)	MS content in CS/($g \cdot kg^{-1}$)	Cement content in CS/%
W	0	0	0	11.8
MS1	5.1	1.7	1.5	11.8
MS2	15.3	5.1	4.5	11.8
MS3	30.6	10.2	9.0	11.8
MS4	61.2	20.4	18.0	11.8

2.2 UCS test

UCS test was carried out for the blocks with 28 days of curing. UCS was measured by an universal testing machine (Model−5105A) with the maximum load capacity of 100 kN and the loading rate of 5 mm/min. The average result from the three tested blocks is used as the block value of UCS.

2.3 XRD

Phase analyses were performed for the cemented

soil samples (Table 2) in powder form after the UCS test using the TD 3500 X-ray diffraction (XRD) machine made in Denmark. Powder samples were ground to pass the sieve diameter of 0.080 mm. The sample was scanned with the scanning angle of 20°−70° and scanning speed of 0.02 (°)/s. After the test, the corrosive powders were analyzed by JADE5.0 software [20] to determine their chemical components.

2.4 SEM and EDS

1) The samples for SEM and EDS were taken from the blocks after the UCS test. The coarse samples were dehydrated in ventilation cabinet and polished by No. 1200 fine sandpapers.

2) In order to enhance the electrical conductivity and get better SEM images, the samples were covered with powdered gold by Small Ion Sputtering Apparatus (SISA, type of SBC−12).

3) The SEM images were taken in HITACHI tabletop microscope (TM3000) and saved as BMP format when the imaging is the clearest by adjusting brightness, contrast, and focal length. In order to avoid repeated focusing, the images were obtained on a continuous scanning model magnified in 200−4000 times.

4) At the same time, for each image, uniform distribution from six sampling sites of the EDS test was assumed under 200 times magnification. The average element content from the six sampling sites is used.

5) SEM images were processed by IPP 6.0 analysis software. The sample SEM images were converted into binary images and the pore information including count, average diameter (AD) of equivalent circle, and pore area was determined.

3 Results and discussion

3.1 UCS test results

UCS values calculated for the cemented soil blocks are shown in Fig. 1. From Fig. 1, it is concluded that:

1) First, UCS value increases with the increase of MS content. Maximum strength of 5.03 MPa is reached when the content of MS is 4.5 g/kg (i.e., Sample MS2), by 10.07% compared with Sample W. The UCS value for Samples MS1 and MS3 is also larger than that for Sample W.

2) UCS decreases when the content of MS is greater than 4.5 g/kg. The UCS value of Sample MS4 is 4.13 MPa, when MS content is 18 g/kg, which is 9.63% lower than that of Sample W.

3) MS content plays an important role in UCS of CS. Therefore, the existing environmental condition of cemented soils should be taken into account when determining the foundation bearing capacity and the settlement for safer, optimal, and more economical designs.

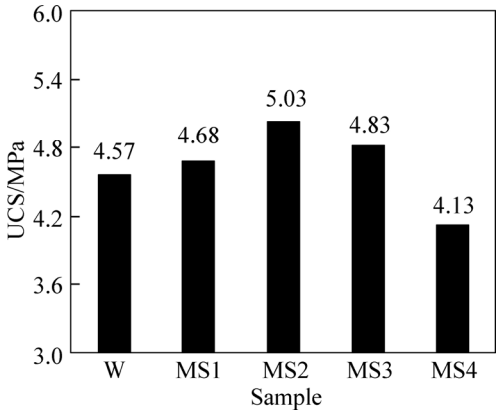

Fig. 1 UCS of cemented soil

3.2 EDS results

EDS results for Samples MS1 and MS4 are shown in Fig. 2. Besides the element distribution diagrams, distribution diagrams for the three elements (i.e., oxygen (O), magnesium (Mg), and sulfur (S)) are also shown in Fig. 2. In each image, the element content from six evenly-spread sampling sites is analyzed. The statistical element contents of MS1 and MS4 are listed in Table 3. From the EDS results, it can be concluded that:

1) Samples MS1 and MS4 mainly contain 10 kinds of other elements besides hydrogen (H) element, which could not be detected by EDS (Fig. 2). These 10 kinds of elements are oxygen (O), silicon (Si), calcium (Ca), aluminum (Al), carbon (C), ferrum (Fe), potassium (K), sodium (Na), magnesium (Mg), and sulfur (S) in the decreasing order of content (Table 3).

2) Because different MS contents are mixed in the cemented soil, there are three elements (i.e., O, Mg and S) studied primarily. When MS content is 1.5 g/kg in CS (Sample MS1), oxygen (O) accounts for 50.33% and the variation coefficient is 0.023 only. Compared with Sample MS1, Sample MS4, whose MS content is 18.0 g/kg, has greater oxygen (O) content and its variation coefficient is also very small (0.033). These demonstrate that oxygen (O) is the greatest element and its distribution is uniform.

Then, from the statistical element distribution data (Table 3), the mean magnesium (Mg) contents are 1.35% for MS1 and 1.73% for MS4. The mean sulfur (S) contents are 0.21% for MS1 and 0.36% for MS4. For these two elements, the content in Sample MS4 is greater than that in Sample MS1. From the variation coefficient values of magnesium (Mg) and sulfur (S), it is seen that the two elements in Samples MS1 and MS4 are unevenly distributed as their variation coefficient values are greater than 0.10.

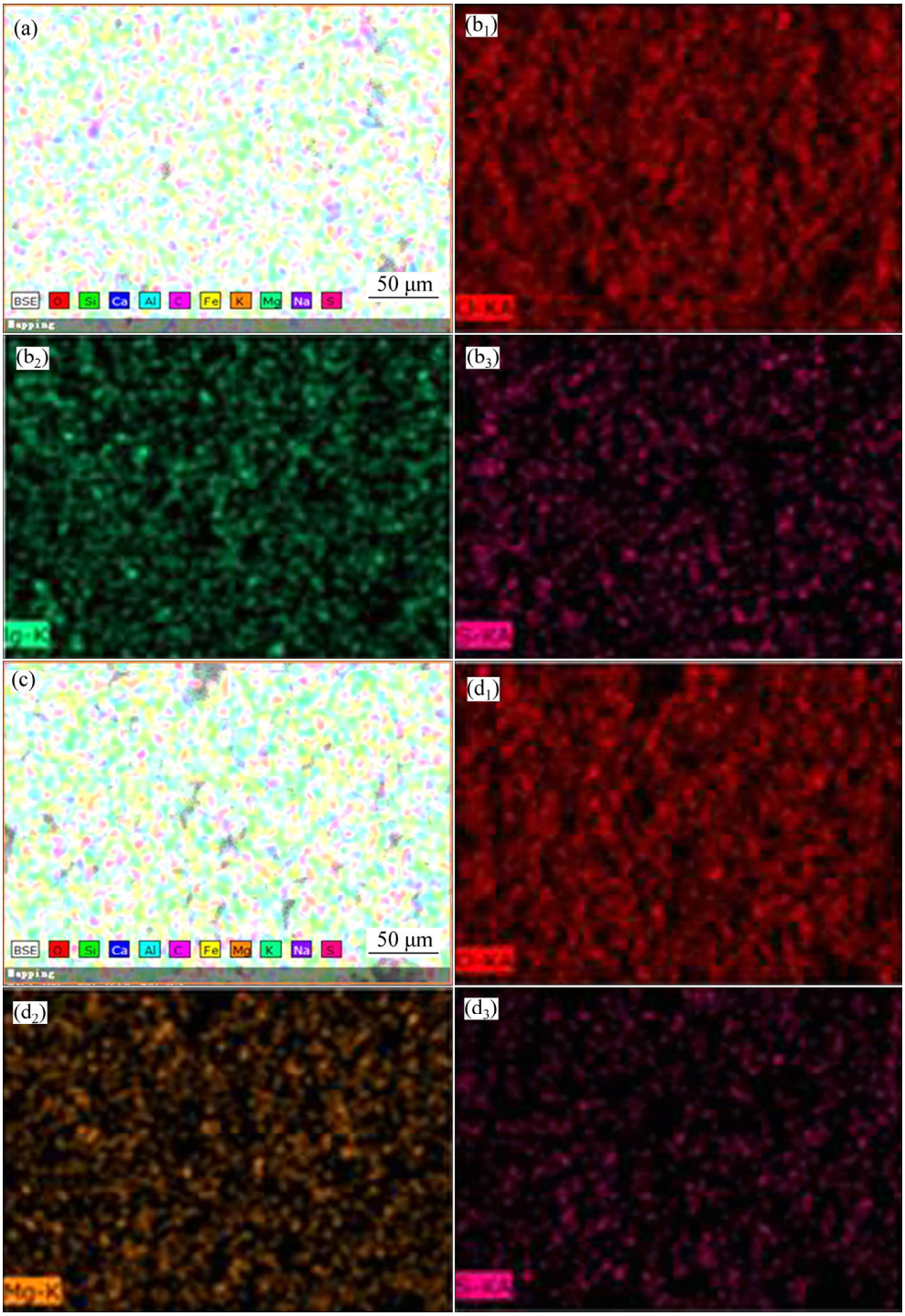

Fig. 2 EDS results: (a) Elements distribution in Sample MS1; (b) Distribution of O (b_1), Mg (b_2) and S (b_3) in Sample MS1; (c) Elements distribution in Sample MS4; (d) Distribution of O (d_1), Mg (d_2) and S (d_3) in Sample MS4

3.3 XRD analysis

Figure 3 gives the XRD patterns of cemented soil with different MS contents. Compared with Sample W, the diffraction peaks of C-A-S-H ($3CaO\cdot Al_2O_3\cdot 3CaSO_4\cdot 32H_2O$ and $3CaO\cdot Al_2O_3\cdot CaSO_4\cdot 18H_2O$), M-A-H ($MgO\cdot Al_2O_3\cdot H_2O$), M-S-H ($MgO\cdot SiO_2\cdot H_2O$), $Mg(OH)_2$, and $CaSO_4$ phase are obviously intense for Samples MS1−MS4. While, the intensity of diffraction peaks for C-S-H ($3CaO\cdot 2SiO_2\cdot 3H_2O$) phase in Samples MS3 and MS4 are lower than those in Sample W (as marked in Fig. 3).

It is generally known that the cement-stabilized soil contains three main chemical reaction processes: hydrolysis and hydration of cement, reaction of silty or clay particles with cement hydrates, and carbonating hardening process for the resulting chemical products. For soils containing MS, in addition to the above three processes, the reactions include

Table 3 EDS analysis results of samples MS1 and MS4

Sample	Statistical parameter	Element in CS samples								
		O	Si	Ca	Al	C	Fe	K+Na	Mg	S
MS1 (6 testing points)	Mean value/%	50.33	17.76	10.53	6.22	5.56	5.48	2.57	1.35	0.21
	Maximum value/%	51.69	19.27	13.18	7.04	7.23	6.72	3.54	1.85	0.30
	Minimum value/%	48.85	14.98	9.52	5.00	3.71	3.75	2.14	0.94	0.15
	Standard deviation	1.18	1.49	1.33	0.80	1.31	1.12	0.51	0.41	0.07
	Variation coefficient	0.023	0.084	0.127	0.129	0.235	0.205	0.200	0.301	0.306
MS4 (6 testing points)	Mean value/%	51.87	18.93	9.42	7.15	4.61	3.89	2.04	1.73	0.36
	Maximum value/%	54.62	20.49	11.61	7.96	6.05	4.16	2.75	2.06	0.44
	Minimum value/%	50.31	16.79	7.92	5.60	1.99	3.56	1.57	1.01	0.26
	Standard deviation	1.72	1.38	1.42	0.85	1.54	0.22	0.43	0.40	0.06
	Variation coefficient	0.033	0.073	0.151	0.119	0.334	0.057	0.213	0.229	0.168

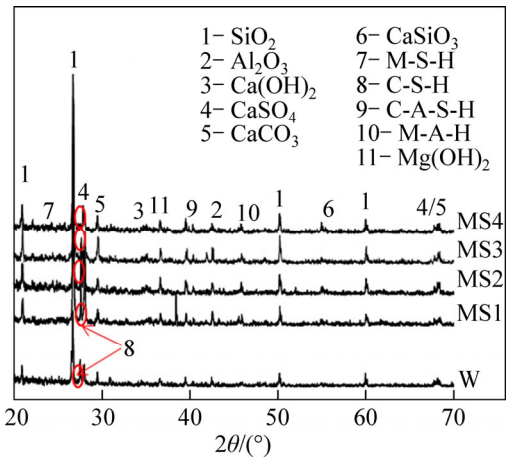

Fig. 3 XRD patterns for samples for 28 days of curing

$$3CaO{\cdot}2SiO_2{\cdot}3H_2O(C\text{-}S\text{-}H)+3MgSO_4+6H_2O=3[CaSO_4{\cdot}2H_2O]+3Mg(OH)_2+2SiO_2 \quad (1)$$

$$3CaO{\cdot}Al_2O_3{\cdot}3H_2O(C\text{-}A\text{-}H)+3MgSO_4+6H_2O=3[CaSO_4{\cdot}2H_2O]+3Mg(OH)_2+Al_2O_3 \quad (2)$$

$$2Mg(OH)_2+3CaO{\cdot}2SiO_2{\cdot}3H_2O(C\text{-}S\text{-}H)=2[MgO{\cdot}SiO_2{\cdot}H_2O](M\text{-}S\text{-}H)+3Ca(OH)_2 \quad (3)$$

$$Mg(OH)_2+3CaO{\cdot}Al_2O_3{\cdot}3H_2O(C\text{-}A\text{-}H)=MgO{\cdot}Al_2O_3{\cdot}H_2O(M\text{-}A\text{-}H)+3Ca(OH)_2 \quad (4)$$

Observed from Eqs. (1) and (2), when there is MS in cemented soil, the chemical reaction develops to dissolve the main cementing agent of CS (i.e., C-S-H and C-A-H) and thus changes the strength of cemented soil. However, the product of $Mg(OH)_2$ appearing in Eqs. (1) and (2), may continue to react with C-S-H and C-A-H chemically, when there is enough $Mg(OH)_2$ in the cemented soil (i.e., Eqs. (3) and (4)). The new reactants such as M-S-H and M-A-H are in poor coagulation and prone to produce an unsteady structure, resulting in reduced strength of cemented soil. Note that Eqs. (3) and (4) are reversible chemical reactions due to the alkaline products of $Ca(OH)_2$ which could not decide the strength of cemented soil. The important influences on the cemented soil strength are

$$3CaSO_4+4CaO{\cdot}Al_2O_3{\cdot}19H_2O+14H_2O=3CaO{\cdot}Al_2O_3{\cdot}3CaSO_4{\cdot}32H_2O+Ca(OH)_2 \quad (5)$$

$$2CaSO_4+3CaO{\cdot}Al_2O_3{\cdot}CaSO_4{\cdot}18H_2O+14H_2O=3CaO{\cdot}Al_2O_3{\cdot}3CaSO_4{\cdot}32H_2O \quad (6)$$

$$CaCO_3+Ca(OH)_2+SiO_2+CaSO_4{\cdot}2H_2O+12H_2O=CaCO_3{\cdot}CaSO_4{\cdot}CaSiO_3{\cdot}15H_2O(C\text{-}C\text{-}C\text{-}H) \quad (7)$$

Those crystallizing resultants, such as $CaSO_4{\cdot}2H_2O$ (from Eqs. (1) and (2)), C-A-S-H (from Eqs. (5) and (6), containing $3CaO{\cdot}Al_2O_3{\cdot}3CaSO_4{\cdot}32H_2O$ and $3CaO{\cdot}Al_2O_3{\cdot}CaSO_4{\cdot}18H_2O$, and C-C-C-H ($CaCO_3{\cdot}CaSO_4{\cdot}CaSiO_3{\cdot}15H_2O$ from Eq. (7)), are more enough than the reactants.

The reason for the strength change due to different MS contents is analyzed hereafter. When the MS content is relatively low (i.e., Samples MS1, MS2 and MS3), the mass of the resulting crystallizing resultants may be suitable to fill in the voids in the cemented soil and is thus beneficial to UCS of CS. This explains why the strength for Samples MS1−MS3 is greater than that of Sample W.

However, the UCS value is lower than any sample value due to the addition of MS. For Sample MS4, on one hand, seen from Eqs. (1)−(4), the new reactants such as M-S-H and M-A-H are in poor coagulation making the inside structure unstable; On the other hand, the inflating force of crystallizing resultants would be greater than the sticking force within the cemented soil. Hence, the expansion may occur in the cemented soil block and the strength would be reduced. This explains why the strength for Samples MS3 and MS4 is lower than that for Sample MS2.

3.4 Pore distribution analysis

SEM images for samples were processed by Image IPP 6.0 software. These images and their binary images are shown in Fig. 4.

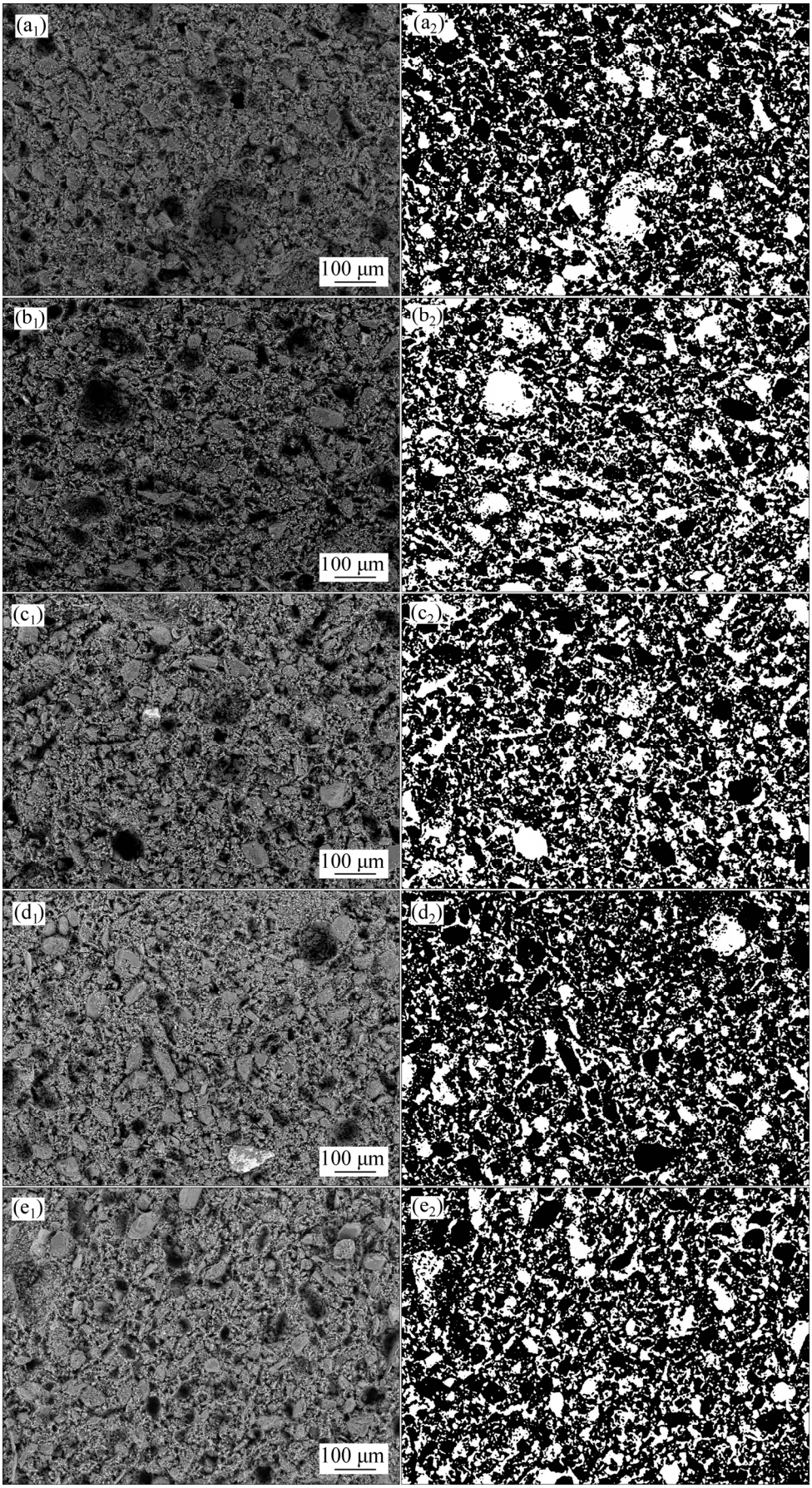

Fig. 4 Original SEM images (a_1−e_1) and binary images (a_2−e_2) processed by IPP 6.0 software: (a_1, a_2) Sample W; (b_1, b_2) Sample MS1; (c_1, c_2) Sample MS2; (d_1, d_2) Sample MS3; (e_1, e_2) Sample MS4

The average diameter ($\overline{D}$) of pores from the SEM images can be classified into five types: hole ($\overline{D}$ > 50 μm), macro pore (20 μm< $\overline{D}$ ≤50 μm), medium pore (5 μm< $\overline{D}$ ≤20 μm), small pore (2 μm< $\overline{D}$ ≤5 μm), and micro pore ($\overline{D}$ ≤2 μm) [21]. Pore distribution and statistics count from the SEM images are listed in Table 4. It can be seen that the pore distribution is changed due to different MS contents.

Table 4 Pore distribution for samples

Sample	Percent of pore/%					Pore count
	<2 μm	2−5 μm	5−20 μm	20−50 μm	>50 μm	
W	3.7	8.8	30.6	26.8	30.1	2873
MS1	3.6	7.7	22.0	41.0	25.8	2378
MS2	4.6	10.7	40.5	35.9	8.4	2522
MS3	5.2	11.9	38.6	32.2	12.1	3049
MS4	3.9	6.8	41.7	34.0	13.6	2459

For holes ($\overline{D}$ >50 μm), the percent of pore (p_{AD}) for Samples MS1−MS4 is less than that for Sample W. Sample MS2 has the lowest p_{AD} value at 8.4%. For macro pores ($\overline{D}$ =20−50 μm), p_{AD} decreases with increasing the MS content. Sample MS3 has the lowest p_{AD} value of 32.2% among the four MS samples, but it is larger than that for Sample W. For medium pores ($\overline{D}$ = 5−20 μm), Sample MS4 (MS content of 18.0 g/kg) has the highest p_{AD} value at 41.7%. For small pores ($\overline{D}$ =2−5 μm) and micro pores ($\overline{D}$ <2 μm), Sample MS3 has the maximum p_{AD} value. Therefore, the pore percent is also changed due to the MS chemical reaction involved.

Figure 5 shows the variations of pore percent with average pore diameter (i.e., 2−5, 2−20 and 2−50 μm), which are most apparent when the content is in the range of 4.5−9.0 g/kg (i.e., MS2 and MS3). For $\overline{D}$ =2−5 μm, MS3 composite proportion is the greatest at 11.9%. For 2−20 μm and 2−50 μm, MS2 proportion is more significant at 51.2% and 87.1%, respectively. The strength of Sample MS2 is the greatest among all cemented soils. This indicates that pores with average diameter of 2−50 μm play more important role in terms of strength. In conclusion, the pore distribution changes with MS content, and the pore distribution change causes different strengths.

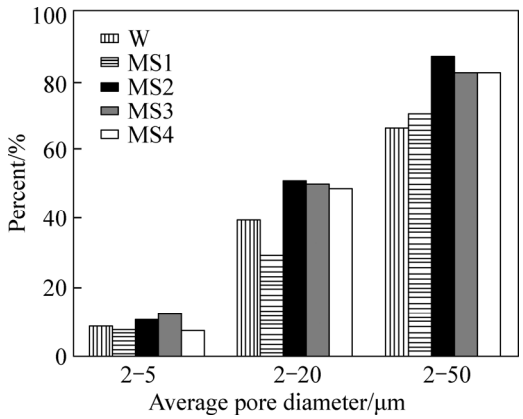

Fig. 5 Percent of pore with different average diameters

3.5 Microstructure and mechanism analysis

Figure 6 shows the microstructures for the samples. It is obvious that the original soil particles are tied with the cement hydration products and form a strong structure of granular-mosaic-cementation. Basically, the microstructure consists of soil particles and flocculation which stick closely to each other (Sample W, Fig. 6(a)). For cemented soils containing MS (i.e., Samples MS1−MS4), there are a large number of granular and crystal particles suspended on the soil sections. The strength of structural system mainly depends on the property of flocculation body.

If the cohesive strength of flocculation bodies is relatively low and the soil particles are arranged loosely, then the soil particles may be accumulated in a state of sliding. Contacting areas are small and the crystal products in flocculation bodies suspending on the soil surface may enhance the strength of cemented soils. However, the degree of such contributing is relatively small (Sample MS1, Fig. 6(b)).

As seen from Figs. 6(c) and (d), for Samples MS2 and MS3, the micro structures contain a large number of bulky crystal products. These crystal products have sticky shapes and fibrous or thick needles distributed in the soil structure. The basic unit of microstructure looks aggregative and clumping. With the increase of the MS content in soils, crystallization continues to inflate and fill the soil voids. The effect of crystallization makes the soil particles cement together closely and changes the particle connection type from sliding to cementing. The bulky crystal products in thick needle shape are C-A-S-H and C-C-C-H, which represent the unique spatial grid structure with hydrolysis and hydration products of cement. This unique structure comprises of soil particles, crystallization products, and other cementing agents in soil voids. It has a stronger strength under loading due to the cohesion of soil particles, especially at the macro level (i.e., Samples MS2 and MS3).

The microstructure of Sample MS4 (Fig. 6(e)), presents the soil particles surrounded by a large number of cementing and crystalline products. But, the strength of cementation mainly from M-A-H and M-S-H is lower than that from C-S-H and C-A-H. Additionally, crystallization products such as C-A-S-H and C-C-C-H surrounding the soil particles are abundant. Soil particle, cementation, and crystallization form the basic unit of the microstructure. Figure 7 shows the microstructure unit, in which one is the original SEM image and the other is the binary image processed by IPP 6.0 software.

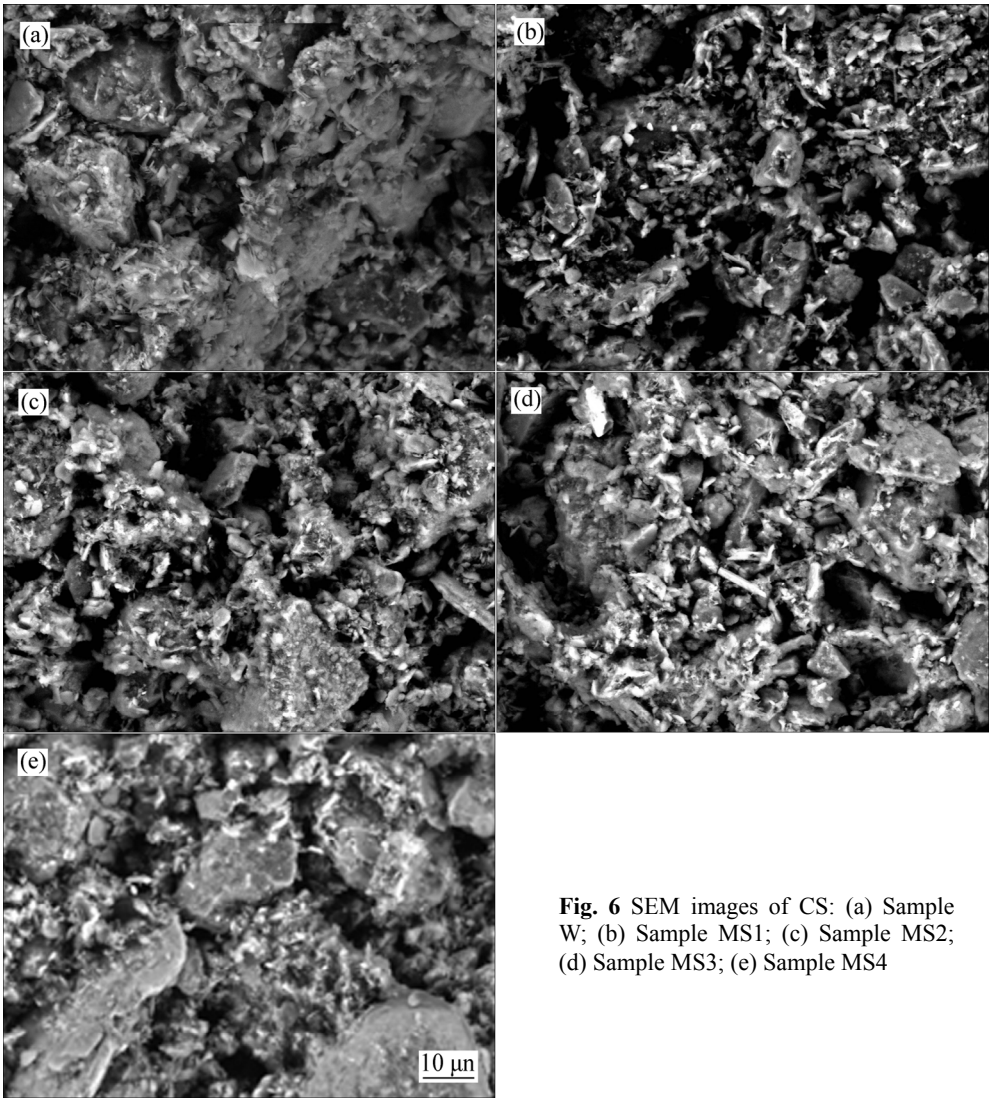

Fig. 6 SEM images of CS: (a) Sample W; (b) Sample MS1; (c) Sample MS2; (d) Sample MS3; (e) Sample MS4

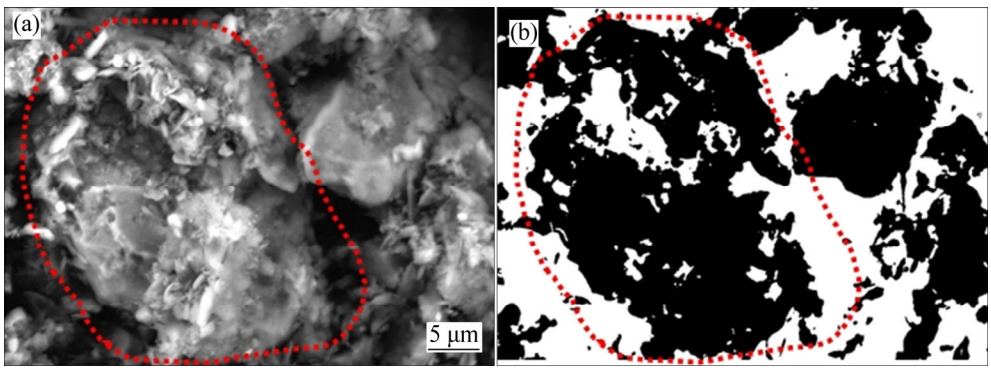

Fig. 7 Comparison of SEM images of Sample MS4: (a) Original SEM image; (b) Binary image

As noted from Fig. 7, compared with Sample MS2 or Sample MS3, the connection type has been changed. Several primary smaller pores start to develop into the interconnected pores. The cohesive strength of soil particles begin to decrease in Sample MS4 due to M-A-H, M-S-H, C-A-S-H, and C-C-C-H products. This strength is relatively low and the structure is easy to be compacted under external loads. This is why the strength of Sample MS4 is lower than that of other samples.

4 Conclusions

1) MS plays an important role in UCS of CS. UCS increases with the increase of MS content. UCS reaches the maximum value when the MS content is 4.5 g/kg (Sample MS2). It decreases when the MS content is

greater than 4.5 g/kg.

2) EDS results of Samples MS1 and MS4 are analyzed. Cemented soils contain 10 kinds of main elements besides hydrogen (H). Oxygen (O) is the most element and its distribution is uniform. From the variation coefficient values of magnesium (Mg) and sulfur (S), it is shown that there are unevenly distributed elements in Samples MS1 and MS4.

3) The XRD pattern shows that the diffraction peaks for the products such as C-A-S-H, M-A-H, M-S-H, $Mg(OH)_2$ and $CaSO_4$ are obviously intense in the samples containing MS. Based on the analysis of chemical reactions, the relationships among UCS, MS content, and chemical products are also established and analyzed.

4) Pore distribution results of SEM images are analyzed. Pore distribution is changed due to MS and the pores with average diameter of 2−50 μm play the important role in the UCS of CS.

5) By combining microstructure of sampling SEM images, mechanism of MS to CS is studied. MS acts as the additive which is beneficial to the strength when the content is low (e.g., Sample MS2). While, larger MS contents involve the chemical action, making the sample crystallize and expand and this is adverse to the UCS growth of CS (e.g., Sample MS4).

References

[1] ROLLINGS R, BURKES J, ROLLINGS M. Sulfate attack on cement-stabilized sand [J]. Journal of Geotechnical and Geoenvironmental Engineering, 1999, 125(5): 364−372.

[2] BAI Xiao-hong, ZHAO Yong-qiang, HAN Peng-ju, QIAO Jun-yi, WU Zhi-an. Experimental study on mechanical property of cemented soil under environmental contaminations [J]. Chinese Journal of Geotechnical Engineering, 2007, 29(8): 1260−1263. (in Chinese)

[3] SHITATA S A, BAGHDADI Z A. Long-term strength and durability of soil cement [J]. Journal of Materials in Civil Engineering, 2001, 13(3): 161−165.

[4] HUANG Yu, ZHOU Zhi-zhou, BAI Tong, CHEN Chi-fen. Micro-experiments in cement-mixed soils on a dredger fill of soft ground [J]. Chinese Journal of Tongji University (Natural Science), 2010, 38(7): 997−1001. (in Chinese)

[5] DONG Xiao-qiang, BAI Xiao-hong, ZHAO Yong-qiang, HAN Peng-ju. Study on electrical resistivity of soil-cement polluted by H_2SO_4 [J]. Chinese Rock and Soil Mechanics, 2007, 28(8): 1453−1548. (in Chinese)

[6] DONG Xiao-qiang, BAI Xiao-hong, LV Yong-kang. The influence of pH value and SO_4^{2-} concentration on strength of cemented soil [J]. Advanced Materials Research, 2011, 223(1): 2006−2010.

[7] XING Hao-feng, YANG Xiao-mging, XU Chao, YE Guan-bao. Strength characteristics and mechanisms of salt-rich soil cement [J]. Engineering Geology, 2009, 103(1/2): 33−38.

[8] LIU Zhi-ping, LIU Quan-sheng, QU Jia-wang, HE Jun. Study on durability of cement soil under brine erosion [J]. Advanced Materials Research, 2012, 446(1): 1858−1863.

[9] HEINECK K S, LEMOS R G, LAUTENSCHLAGER C E R, CONSOLI N C. Behavior of vertical hydraulic barriers composed by sandy soil, bentonite and cement subjected to alkaline contaminants [J]. Geotechnical Special Publication, 2010, 199(2): 2462−2471.

[10] VOGLAR G E, LESTAN D. Efficiency modeling of solidification/stabilization of multi-metal contaminated industrial soil using cement and additives [J]. Journal of Hazardous Materials, 2011, 192(2): 753−762.

[11] ZHA Fu-sheng, LIU Jing-jing, XU Long, CUI Ke-rui. Effect of cyclic drying and wetting on engineering properties of heavy metal contaminated soils solidified/stabilized with fly ash [J]. Journal of Central South University, 2013, 20(7): 1947−1952.

[12] ZANDIEH A R, YASROBI S S. Study of factors affecting the compressive strength of sandy soil stabilized with polymer [J]. Geotechnical and Geological Engineering, 2010, 28(2): 139−145.

[13] WALKER P J. Strength durability and shrinkage characteristics of cement stabilized soil blocks [J]. Cement and Concrete Composites, 1995, 17(4): 301−310.

[14] WALKER P J, DOBSON S. Pullout tests on deformed and plain rebar in cement-stabilized rammed earth [J]. Journal of Materials in Civil Engineering, 2001, 13(4): 291−297.

[15] NING Bao-kuan, CHEN Si-li, LIU Bin. Fracturing behaviors of cemented soil under environmental erosion [J]. Chinese Rock and Soil Mechanics, 2005, 24(10): 1778−1782. (in Chinese)

[16] NING Bao-kuan, JIN Shen-ji, CHEN Si-li. Influence of erosive ions on mechanical properties of cemented soil [J]. Journal of Shenyang Technology University, 2006, 28(2): 178−181. (in Chinese)

[17] BLASCO N I, DURAN A, SIRERA R, FERNANDEZ J M, ALVAREZ J I. Solidification/stabilization of toxic metals in calcium aluminate cement matrices [J]. Journal of Hazardous Materials, 2013, 260(15): 89−103.

[18] YANG Yu-you, WANG Gui-he, XIE Si-wei. Effect of magnesium sulfate on the unconfined compressive strength of cement treated soils [J]. Journal of Testing and Evaluation, 2012, 40(7): 1−8.

[19] YANG Yu-you, WANG Gui-he, XIE Si-wei, TU Xiao-ming, HUANG Xue-gang. Effect of mechanical property of cemented soil under the different pH value [J]. Applied Clay Science, 2013, 79(7): 19−24.

[20] WANG Pei-ming, XU Qian-wei. Materials research methods [M]. Beijing: Chinese Science Press, 2005: 70−71. (in Chinese)

[21] CUI De-shan, XIANG Wei. Pore diameter distribution test of red clay treated with ISS [J]. Chinese Rock and Soil Mechanics, 2010, 31(10): 3096−3100. (in Chinese)

(Edited by YANG Bing)